

# Catch and Release: Orbital Symmetry Guided Reaction Dynamics from a Freed “Tension Trapped Transition State”

Junpeng Wang,<sup>†</sup> Mitchell T. Ong,<sup>‡</sup> Tatiana B. Kouznetsova,<sup>†</sup> Jeremy M. Lenhardt,<sup>‡</sup> Todd J. Martínez,<sup>\*,§</sup> and Stephen L. Craig<sup>\*,†</sup>

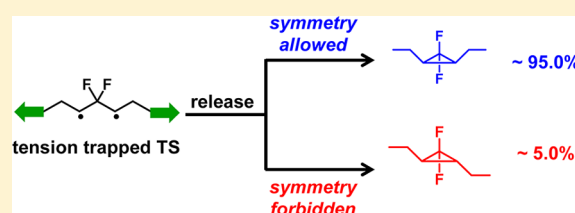
<sup>†</sup>Department of Chemistry, Duke University, Durham, North Carolina 27708, United States

<sup>‡</sup>Materials Science Division, Lawrence Livermore National Laboratory, Livermore, California 94550, United States

<sup>§</sup>Department of Chemistry, Stanford University, Stanford, California 94305, United States

## S Supporting Information

**ABSTRACT:** The dynamics of reactions at or in the immediate vicinity of transition states are critical to reaction rates and product distributions, but direct experimental probes of those dynamics are rare. Here, *s-trans*, *s-trans* 1,3-diradicaloid transition states are trapped by tension along the backbone of purely *cis*-substituted *gem*-difluorocyclopropanated polybutadiene using the extensional forces generated by pulsed sonication of dilute polymer solutions. Once released, the branching ratio between symmetry-allowed disrotatory ring closing (of which the trapped diradicaloid structure is the transition state) and symmetry-forbidden conrotatory ring closing (whose transition state is nearby) can be inferred. Net conrotatory ring closing occurred in  $5.0 \pm 0.5\%$  of the released transition states, in excellent agreement with *ab initio* molecular dynamics simulations.



## ■ INTRODUCTION

Reaction dynamics in the vicinity of transition states are intrinsically tied to reaction mechanisms and product distributions. Understanding those dynamics, and if/how they are influenced by the trajectory that brought the molecule to that point, is therefore of significant interest. To that end, it is desirable to know the intrinsic dynamics of transition states, i.e., how a reaction proceeds if a molecule is dropped right at the transition state, and to compare observations to predictions based on molecular simulations and/or transition-state theory. To date, the experimental observations of transition-state structure and dynamics are based either on a characterization of product energy levels through scattering experiments, such as those performed by Polanyi<sup>1</sup> and Brooks,<sup>2</sup> the time-resolved pump–probe “femtochemistry” experiments pioneered by Zewail,<sup>3</sup> or the negative ion photodetachment experiments of Neumark<sup>4</sup> and Lineberger.<sup>5</sup> The dynamics in question tend to focus on a single trajectory as the activated complex descends toward product from either side of the (often symmetrical) dividing surface. Studies involving branching between non-degenerate pathways, for example, those accessed through an additional dividing surface near that on which the activated complex resides, are rare. Here, we investigate branching reaction dynamics in the context of the ring-closing reaction of a 2,2-difluoro-1,3-diyl whose propensity for conrotatory vs disrotatory closure is influenced by orbital symmetry effects that underlie the famous Woodward–Hoffmann rules.<sup>6</sup>

In recent years, covalent mechanochemistry has been explored as a new methodology for studying reaction mechanisms.<sup>7</sup> To this end, various methods have been

developed to probe force-coupled reactions,<sup>8</sup> including single-molecule force spectroscopy,<sup>9–11</sup> pulsed ultrasonication,<sup>12</sup> Boulatov’s molecular probes,<sup>13</sup> and Matyjaszewski and Sheiko’s bottle brush polymers.<sup>14</sup> Among these techniques, the use of pulsed sonication of polymer solutions is advantageous in that the experiments are operationally straightforward and the products of force-coupled reactions can be conveniently characterized by conventional spectroscopic techniques. During sonication, elongational flow fields are generated by cavitation, which includes the nucleation, growth, and collapse of microbubbles.<sup>15</sup> A velocity gradient is then formed in the direction of a collapsing bubble; the polymer segments that are closer to the bubble have a higher velocity than those farther from the bubble,<sup>15</sup> and the polymer is thus stretched and elongated. The midchain of the polymer is typically where the highest force is located and where chain scission occurs.<sup>9</sup>

Sonication mechanophore-embedded polymers provides an opportunity to probe the mechanochemical response of the molecules in solution, and we have recently used sonication to demonstrate the concept of tension trapping,<sup>16</sup> in which transition states and high-energy intermediates are stabilized as global minima on force-coupled potential energy surfaces.<sup>16</sup> The force is delivered by overstressed polymer “handles,” and tension trapping has been applied to carbonyl ylides<sup>17</sup> and to the 1,3-diradicaloid transition state of *gem*-difluorocyclopropane

**Special Issue:** 50 Years and Counting: The Woodward–Hoffmann Rules in the 21st Century

**Received:** July 1, 2015

**Published:** August 31, 2015

(gDFC) isomerization,<sup>16</sup> enabling unexpected isomerizations,<sup>16,17</sup> intermolecular chemical trapping of the dynamically trapped species,<sup>16,17</sup> and new, intramolecular reactions between multiple transition states trapped in proximity.<sup>18</sup> Here we explore what happens when the 1,3-diradicaloid is released (Figure 1).

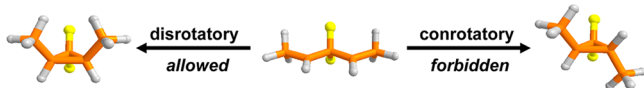


**Figure 1.** A released 2,2-difluoro-1,3-diyl can close either along the disrotatory process of which it is a transition state or surmount a higher barrier to close in a conrotatory fashion.

The diradicaloid, a 2,2-difluoro-1,3-diyl, corresponds to the transition state of the force-free, disrotatory *cis*-to-*cis* inversion of gDFC,<sup>19</sup> but a nearby, higher energy transition state associated with conrotatory ring closing to the *trans* gDFC also exists. The preference for the disrotatory process has been characterized by Borden and co-workers<sup>20</sup> and is a result of orbital symmetry effects;<sup>6</sup> the 2  $\pi$ -electron nature of the system is attributed to the electron-withdrawing character of the fluorines. These ring-closing dynamics lead to a counter-intuitive result: there is a net contraction in length along the affected regions of the polymer backbone in response to a force of tension (the polymer grows shorter once it is pulled), and the products are higher in energy than the reactants, as there is a net conversion of *trans*-gDFC to *cis*-gDFC.<sup>11</sup> It is clear from the prior studies that the vast majority of the released diradicaloids closed via a disrotatory motion, but we set out to quantify the small fraction of ring-closing reactions that occurred via a net conrotatory motion, thus directly probing the reaction dynamics in the vicinity of the transition-state dividing surface.

## RESULTS AND DISCUSSION

The experimental design is shown in Figure 2. Ring-opening metathesis polymerization<sup>21</sup> (ROMP) of difluorocyclopropanated cyclooctadiene **1** yielded gDFC polybutadiene (PB) **2**. The methodology gave a polymer with only *cis*-connected gDFCs along its backbone, which allowed us to quantify the formation of very small levels of *trans*-gDFC that might have been obscured by the nascent *trans* content in previous studies.<sup>11</sup> Polymer **2** was then subjected to pulsed ultrasonication (30% amplitude, 11.9 W/cm<sup>2</sup>), conditions previously shown to mechanically force the gDFCs to open into trapped 1,3-diradicaloid transition states.<sup>11</sup> After 60 min of sonication, the molecular weight was reduced from 115 to 54 kDa, and low levels (2%) of *cis*-to-*trans* isomerization were observed by <sup>19</sup>F NMR (**4**, Figure 2).

In order to occur in pulsed ultrasound, the time scale of a mechanochemical reaction must be comparable to, or shorter than, the time scale of the extensional flow event that generates the tension ( $\sim 10^{-8}$ – $10^{-6}$  s).<sup>22</sup> Thus, the force-coupled activation energy for *cis*-to-*trans* gDFC isomerization under these conditions must be  $< \sim 9$  kcal mol<sup>-1</sup>. There is a distribution of forces along each activated polymer chain, and our calculations show that the force necessary to lower the activation energy to this extent is also sufficient to stabilize the 1,3-diradicaloid as a global minimum on the force-coupled potential energy surface.<sup>11</sup> Within the range of force experienced, those mechanophores that experience sufficient

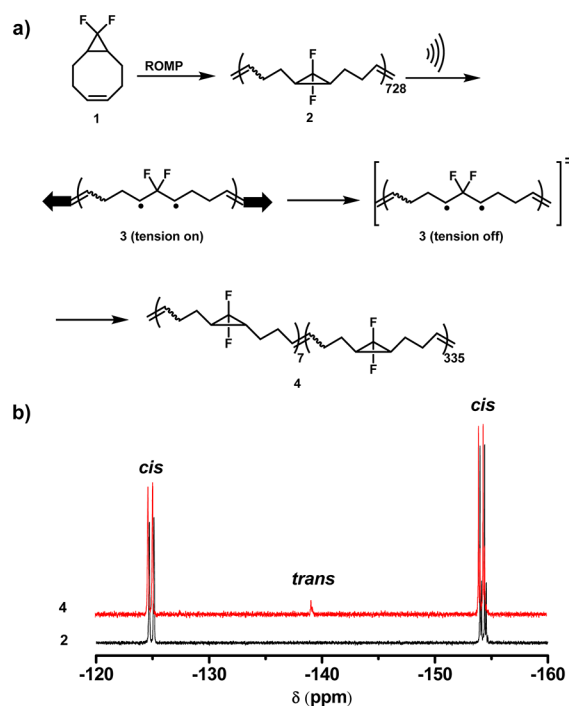


**Figure 2.** (a) Ring-opening metathesis polymerization of **1** generates pure *cis*-gDFC-PB **2**, which was sonicated in dilute solution for 1 h. When force is applied to **2**, diradicaloid transition-state structures **3** are trapped under tension as global minima on the force-coupled potential energy surface. When the force is released, **3** is converted to a true transition-state saddle point, and ring closure occurs rapidly in either a disrotatory or conrotatory manner to form copolymer **4**. (b) <sup>19</sup>F NMR of **2** (bottom, black) and **4** (top, red): the peaks at -125 and -154 ppm correspond to *cis*-gDFC, while the peak at -139 ppm corresponds to *trans*-gDFC.

force to be opened must also experience sufficient force to be trapped as a diradicaloid. In other words, direct mechanochemical *cis*-to-*trans* isomerization is not possible in these experiments, and so when *trans*-gDFC is observed, it must have been formed from trapped transition states that close once the tension is released.

We can therefore quantify the number of disrotatory ring-closing reactions, and so in order to quantify the probability of disrotatory closure, we need only to know how many 1,3-diradicaloids were trapped and subsequently released. Because most diradicals close back to the original *cis* configuration, direct measures of ring opening are not available. The extent of ring opening can be gauged fairly accurately by comparison to similar systems, in particular the mechanochemical ring opening of *gem*-dichlorocyclopropanes (gDCC).<sup>23</sup> Although the reaction outcomes are different, the activation energies and transition-state geometries for gDCC and gDFC ring opening are similar, and the extents of sonochemical ring opening of the two *trans* isomers are indistinguishable.<sup>24</sup> In addition, we have recently found that the threshold forces for mechanochemical ring opening of *cis*-gDCC and *cis*-gDFC are very similar (in fact, closer than those of the corresponding *trans* isomers that are themselves effectively indistinguishable in sonication), as measured by single molecule force spectroscopy (time scale  $\sim 100$  ms).<sup>25</sup> When the force-rate relationship derived from the force spectroscopy is extrapolated to the time scale of sonication ( $10^{-8}$  s), it is determined that the force required to activate *cis*-gDFC is nearly indistinguishable from that

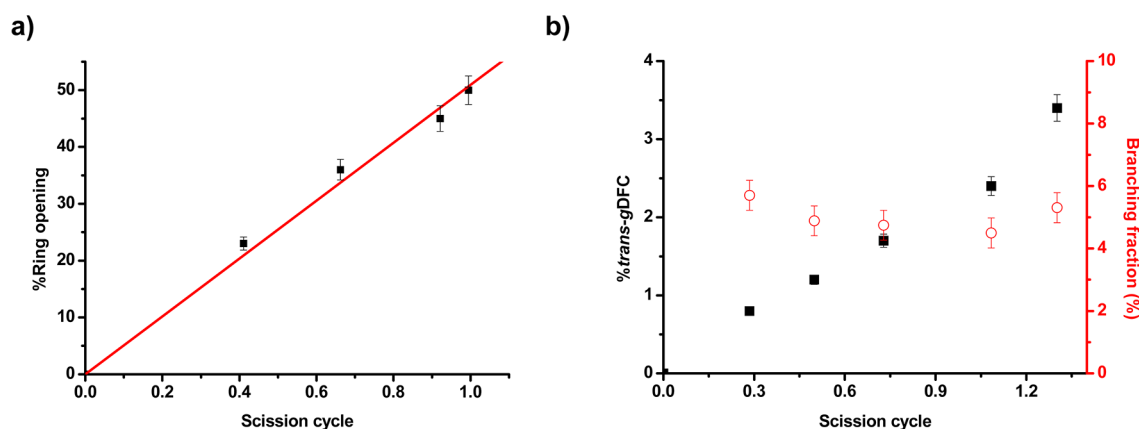


**Figure 3.** (a) Sonication of gDCC polymer (1 mg/mL in THF, 6–9 °C, N<sub>2</sub> atmosphere). The ring-opening percentage was characterized from <sup>1</sup>H NMR and plotted against scission cycle. (b) Sonication of polymer 2 (1 mg/mL in THF, 6–9 °C, N<sub>2</sub> atmosphere). The percentage of *trans*-gDFC (black filled square, characterized from <sup>19</sup>F NMR) and branching fraction (red empty circle) were plotted against scission cycles. The branching fractions are determined from the ratio of the percentage of *trans*-gDFC to the percentage of the ring opening of *cis*-gDCC at certain scission cycles.

required to activate *cis*-gDCC (2290 vs 2370 pN, respectively; see Supporting Information (SI)).

We therefore synthesized a 123 kDa *cis*-gDCC-PB and subjected it to sonication conditions that are identical to those used for the gDFC-PB. The ring opening and molecular weight at different time intervals were characterized by <sup>1</sup>H NMR and gel permeation chromatography (GPC), respectively. As shown in Figure 3a, there is a linear relationship between gDCC ring opening and the scission cycle (SC, where SC = (ln *M*<sub>n(o)</sub> – ln *M*<sub>n(t)</sub>)/(ln 2)). One scission cycle is the point at which the polymer *M*<sub>n</sub> is cut in half, two scission cycles where it has been reduced to 1/4 its initial value, etc.). The data are fit by the following line:

$$\text{Fraction of ring opening} = 0.51 \times \text{SC} \quad (1)$$

The *M*<sub>n</sub> of polymer 2 was therefore monitored as a function of sonication time, and the percentage of activated gDFC was estimated using eq 1. The *trans*-gDFC content of the polymers increased linearly with scission cycle (Figure 3b), and the probability of net conrotatory ring-closing is given by the ratio of the fraction of total rings that closed to *trans*-gDFC (from <sup>19</sup>F NMR) to the fraction of total rings that opened (from eq 1). As shown in Figure 3b, the branching fraction remained constant (5.0 ± 0.5%) over the data reported.

The fact that the branching fraction stays constant is significant, because a given gDFC can theoretically be activated multiple times. Of course, only the fate of the last ring opening/closing is reported, and since *trans*-gDFC is less reactive than the *cis* isomer,<sup>25</sup> it is possible for *trans*-gDFC to turn into a sort of kinetic sink as the original gDFCs undergo repeated activations. If such contributions were significant, they would be revealed by an increase in the conrotatory branching fraction with reaction time. The fact that the branching fraction remained constant suggests that such contributions are not significant over the range of times employed, and so the branching fraction is indicative of the “true” branching fraction of the reactants. We note that with even longer sonication times, however, the branching fraction does start to increase as expected (see SI), but we rely on the data in the “constant branching fraction” time interval for our interpretation.

The overall *cis* to *trans* isomerization is caused by conrotatory ring closing or monorotation followed by disrotatory ring closing, meaning that 5.0 ± 0.5% of all released transition states

undergo either conrotation or monorotation. The results and ensuing dynamical picture are summarized in Figure 4. We compared this result to that obtained from molecular dynamics (MD) simulations<sup>26</sup> on the parent gDFC diradicaloid,<sup>11</sup> trapped using simulated trapping forces of 2 and 3 nN and then released. Our best estimate of the singlet–triplet gap at the disrotatory transition state is >4 kcal mol<sup>–1</sup> (see SI). Thus,

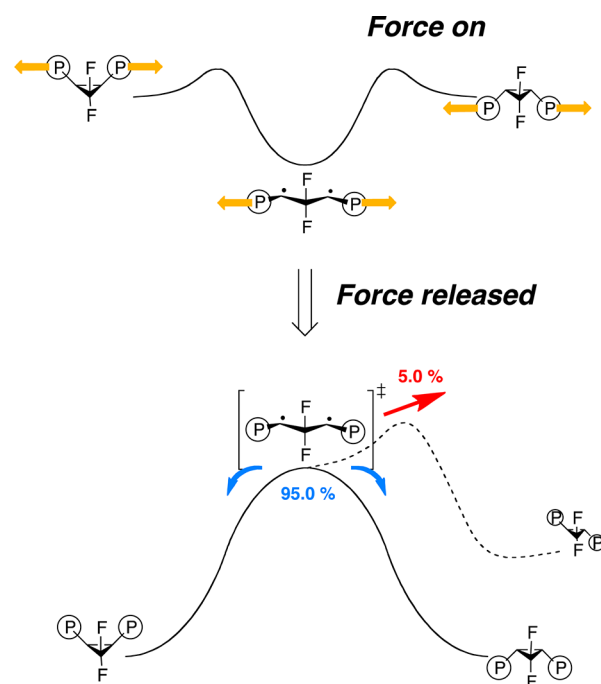


**Figure 4.** Ring-closing dynamics of a freed tension trapped transition state. Under tension applied by mechanochemical polymer extension (top), the 1,3-diradicaloid is trapped as a global minimum on the reaction potential energy surface. When the tension is released (bottom), the same diradicaloid structure is now the transition state along the force-free isomerization pathway of *cis*-gDFCs, but 5.0 ± 0.5% of the released structures surmount a nearby, additional barrier and close instead to the *trans* isomer. Note that the *trans* isomer could be formed from either direct conrotatory ring closing or a net conrotatory ring closing via sequential monorotation followed by disrotatory ring closing. The enantiomeric conrotatory closing and monorotatory pathways are not shown for clarity.

our MD simulations were restricted to the singlet surface. A total of 400 trajectories were computed (200 each at 2 and 3 nN). We observed that 17 of the 400 trajectories closed in a direct symmetry forbidden conrotatory fashion, and an additional 2 of the 400 underwent net conrotatory ring closing via sequential monorotation followed by disrotation. The total net conrotatory ring-closing branching fraction of  $4.75 \pm 2\%$  (19/400) is within statistical uncertainty of the experimental branching ratio.

The observed 19:1 branching ratio between the disrotatory and conrotatory pathways is smaller than that predicted by transition-state theory for a difference in activation energies of 4 kcal/mol<sup>11</sup> ( $\sim 1300:1$  at 280 K). It is also smaller than the reported 107:1 ratio between *cis*-gDFC racemization and *cis*-to-*trans* isomerization observed in the thermally promoted stereomutations of *cis*-substituted gDFCs.<sup>19</sup> These observations are reminiscent of those noted previously by Carpenter in MD simulations of the thermal interconversion of bicyclo[2.2.1]-hept-2-ene.<sup>27</sup> In that case, the lifetime of the biradical intermediate showed a bimodal distribution; 10 of the 100 trajectories passed through the transition state and exited in 250–350 fs, whereas the rest failed to take the exit directly and their lifetime was extended to 0.1 ns. The short-lived intermediates yielded only inversion product, and the long-lived trajectories formed both inversion and retention products in a ratio of 1:1. The difference in the product distributions was attributed to dynamic effects in the short-lived trajectories due to initial inertia.<sup>27</sup> Similar inertial effects could be at play for the force-free isomerization of gDFC: the inertia of disrotatory ring opening might channel the reactant toward a disrotatory ring-closing process.<sup>28</sup> In the tension trapping experiments, however, the trapping would effectively negate any memory of the initial ring-opening trajectory, so that conrotatory ring closing would be more prevalent than in the force-free case.

An alternative explanation involves the dynamics associated with the release of tension. The force does not instantaneously drop from that required for trapping ( $>2$  nN) to zero; there is a time scale associated with the disappearance of the force. A reasonable consideration, therefore, is how much force still remains on the system when the ring closure occurs, as that force could bias the ring closing outcome. The calculated force-modified potential energy surface for the perhydro-gDFC (see SI) shows that the observed disrotatory ring closing is favored only at low force. To have a selectivity of  $\sim 20:1$  or greater, the activation energy for disrotatory ring closing needs to be at least  $\sim 2$  kcal/mol lower than that for conrotatory ring closing. The disrotatory ring-closing barrier only drops below the conrotatory ring-closing barrier when the absolute barriers for ring closing are 2–4 kcal/mol (see SI), and the time scale for closing would be on the order of ps. It seems possible to us that the time scale of force dissipation could be similar. In distinguishing between these possibilities, we note that the branching fraction obtained from MD simulations ( $4.75 \pm 2\%$ ) agrees well with the experimental results ( $5.0 \pm 0.5\%$ ), and in those simulations the force is released instantly. That agreement suggests that the reaction inertia effects might be more significant.

Finally, we note that when the force disappears, a substantial amount of energy stored in enthalpic distortions of the polymer is released. That energy is initially transferred into kinetic energy of the atoms along the polymer backbone. In other words, the diradicaloid emerges from the release of force “hot,” and ring closure might occur so quickly that the energy is not

redistributed into the surroundings. As a consequence, the effective temperature of the reactant at which the ring closing occurs might be substantially higher than the temperature of the solvent, and that temperature might contribute to the reduced selectivity.

## CONCLUSION

While the exact relationship to the dynamics of analogous force-free reactions is not clear, this study provides a first glimpse into reaction dynamics in the vicinity of the transition state of reaction whose selectivity is controlled by the orbital symmetry effects first explained by Woodward and Hoffmann 50 years ago.<sup>6</sup> The approach described here expands the utility of mechanochemical methods as a tool for reaction engineering,<sup>12,29–33</sup> and it provides a rare experimental probe of the dynamics that can be simulated computationally in the vicinity of transition states, a topic that has received considerable attention recently. In the case of the tension trapped diradicaloid, a significant ( $\sim 5.0\%$ ) fraction of the released transition states surmount an additional reaction barrier of approximately 4 kcal/mol<sup>11</sup> (conrotation along the symmetry “forbidden” conrotatory pathway) or 6.6 kcal/mol (monorotation),<sup>19</sup> rather than taking the barrierless or nearly barrierless trajectory down the symmetry allowed conrotatory ring closing.

The details that lead to those dynamics remain somewhat speculative, but at a minimum the results obtained here suggest that the *s-trans*, *s-trans* 1,3-diradicaloid transition state of the disrotatory ring opening is a competent intermediate structure along the *cis*-to-*trans* isomerization pathway; a given reaction trajectory might pass through both dividing surfaces, rather than immediately rolling energetically downhill after surmounting the first summit. The relatively high level of branching to the conrotatory pathway also raises the intriguing possibility that more subtle dynamical contributions might be at play in tension trapping, for example, those due to competition between relaxation of the previously overstrained conformations (i.e., the rate at which the force goes to zero) and the dynamics of nuclear motion along the available reaction coordinates. Further characterization of the ultrafast dynamics at play in this and related systems might offer promise not only in testing fundamental notions of reaction dynamics but also offer an opportunity through which the outcomes of chemical reactions can be steered toward unconventional products.

## EXPERIMENTAL SECTION

**General Procedures.** Unless otherwise stated, all starting materials and reagents were purchased from commercial source and used as received. <sup>1</sup>H NMR, <sup>13</sup>C NMR, and <sup>19</sup>F NMR analysis were conducted on a 400 MHz spectrophotometer, and the residual solvent peaks (CDCl<sub>3</sub>, 7.26 ppm [<sup>1</sup>H], 77.16 ppm [<sup>13</sup>C]) were used as an internal chemical shift reference. <sup>19</sup>F spectra were indirectly referenced via the deuterium lock signal of CDCl<sub>3</sub> using the respective reference frequencies ratio as recommended.<sup>34</sup> All chemical shifts are given in ppm ( $\delta$ ) and coupling constants (*J*) in Hz as singlet (s), doublet (d), triplet (t), quartet (q), multiplet (m), or broad (br). Gel permeation chromatography (GPC) experiments were performed on an in-line two columns ( $10^4$  and  $10^3$  Å) using THF (inhibitor free) as the eluent. Molecular weights were calculated using a multi-angle light scattering (MALS) detector and interferometric refractometer (RI). The refractive index increment ( $dn/dc$ ) values were determined by online calculation using injections of known concentration and mass.



**Synthesis.** Monomers (Z)-9,9-difluorobicyclo[6.1.0]non-4-ene (1) and (Z)-9,9-dichlorobicyclo[6.1.0]non-4-ene (5) were synthesized according to literature procedures.<sup>35,36</sup>

**Synthesis of gDFC-PB (2).** 1 (0.3 g, 1.90 mmol) was dissolved in 0.5 mL DCM and deoxygenated with N<sub>2</sub> for 15 min. 1.6 mg (0.0019 mmol) Grubbs second-generation catalyst was dissolved in 1.25 mL DCM and deoxygenated for 20 min. 0.5 mL of the Grubbs catalyst solution was transferred to the monomer solution via a syringe. The viscosity of the solution increased over 20 min, at which point the stirring ceased quickly. One mL of DCM was added to the solution to allow the stirring to continue, and the reaction was allowed to proceed for another 1 h. The reaction was quenched with 1 mL of ethyl vinyl ether and stirred for 1 h. The reaction was then precipitated in methanol, dissolved again in DCM, reprecipitated in methanol, and dried on a vacuum line. <sup>1</sup>H NMR (400 MHz, CDCl<sub>3</sub>) δ 5.54–5.30 (m, 2H), 2.18–1.98 (m, 4H), 1.56–1.32 (m, 6H); <sup>19</sup>F NMR (376 MHz, CDCl<sub>3</sub>) δ –124.89 (dd, *J* = 156.5, 14.6 Hz), –154.26 (dd, *J* = 155.0, 52.9 Hz). *M<sub>n</sub>* = 115,000, PDI = 1.56, *dn/dc* = 0.050 mL/g.

**Synthesis of gDCC-PB (6).** 5 (0.15 g, 1.90 mmol) was dissolved in 0.3 mL DCM and deoxygenated with N<sub>2</sub> for 15 min. 1.1 mg (0.0013 mmol) Grubbs second-generation catalyst was dissolved in 1.0 mL DCM and deoxygenated for 20 min. 0.4 mL of the Grubbs catalyst solution was transferred to the monomer solution via a syringe. The viscosity of the solution increased over 20 min, at which point the stirring ceased to be effective. 0.3 mL of DCM was added to the solution to allow the stirring to continue, and the reaction was allowed to proceed for another 1 h. The reaction was quenched with 0.5 mL of ethyl vinyl ether and stirred for 1 h. The reaction was then precipitated in methanol, dissolved again in DCM, reprecipitated in methanol, and dried on a vacuum line. <sup>1</sup>H NMR (400 MHz, CDCl<sub>3</sub>) δ 5.75–5.21 (m, 2H), 2.48–1.82 (m, 4H), 1.70–1.08 (m, 6H). *M<sub>n</sub>* = 123,000, PDI = 1.52, *dn/dc* = 0.125 mL/g.

**Sonication.** Sonication experiments were performed in inhibitor-free THF on a Vibracell Model VCX 500 operating at 20 kHz with a 12.8 mm titanium tip probe from Sonics and Materials (<http://www.sonics.biz/>). Each sonication was performed on 1 mg/mL polymer solution in ~15 mL of THF. Prior to sonication, the solution was transferred to a 3-neck Suslick cell in an ice bath and deoxygenated by bubbling through nitrogen for 30 min. Irradiations were performed at 11.9 W/cm<sup>2</sup> with a pulse sequence of 1s on/1s off while maintaining a temperature of 6–9 °C under a nitrogen atmosphere.

**Sonication of 2.** A 1 mg/mL THF solution of 2 was sonicated for 1 h to yield 4. <sup>1</sup>H NMR (400 MHz, CDCl<sub>3</sub>) δ 5.58–5.34 (m, 2H), 2.32–1.95 (m, 4H), 1.66–1.18 (m, 6H); <sup>19</sup>F NMR (376 MHz, CDCl<sub>3</sub>) δ –122.19 to –125.96 (m), –136.98 to –142.43 (m), –152.32 to –156.09 (m). *M<sub>n</sub>* = 54,000, PDI = 1.42, *dn/dc* = 0.050 mL/g. The content of *trans*-gDFC can be determined from either <sup>19</sup>F-NMR (0.04/(1 + 0.97 + 0.04) = 2.0%) or <sup>1</sup>H NMR ((0.57 – 1.60/3)/2 = 1.8%); *cis*-gDFC content: 98.0%. Number of repeating units: 54,000/158 = 342; number of *trans*-gDFC: 342 × 2.0% = 7; number of *cis*-gDFC = 335.

**Ab Initio MD Simulations.** Ab initio MD is carried out on the force-modified potential energy surface (FMPES),<sup>26</sup> where the FMPES is computed on the fly with the complete active space self-consistent field (CASSCF) method<sup>37</sup> with second-order perturbative corrections (CASPT2).<sup>38</sup> The active space has two electrons in two orbitals, i.e., CAS(2/2)-PT2, and the 6-31G\* electronic basis set is used. We simulate the dynamics following force release by sampling initial conditions (positions and velocities) from a Wigner distribution at 280 K corresponding to the diradical minimum on the FMPES at 2 or 3 nN. Evolution of these initial conditions then occurs on the force-free potential energy surface until the ring has closed and the reaction pathway can be discerned.

## ■ ASSOCIATED CONTENT

### ● Supporting Information

The Supporting Information is available free of charge on the ACS Publications website at DOI: 10.1021/acs.joc.5b01493.

NMR spectra and GPC-MALS data; calculation of ring-opening forces during sonication; MD simulation details (PDF)

## ■ AUTHOR INFORMATION

### Corresponding Authors

\*E-mail: [todd.martinez@stanford.edu](mailto:todd.martinez@stanford.edu).

\*E-mail: [stephen.craig@duke.edu](mailto:stephen.craig@duke.edu).

### Notes

The authors declare no competing financial interest.

## ■ ACKNOWLEDGMENTS

This material is based on work supported by the U.S. Army Research Laboratory and the Army Research Office under Grant W911NF-07-0409. Part of this work was performed under the auspices of the U.S. Department of Energy by Lawrence Livermore National Laboratory under Contract DE-ACS2-07NA27344.

## ■ REFERENCES

- (1) Arrowsmith, P.; Bartoszek, F. E.; Bly, S. H. P.; Carrington, T.; Charters, P. E.; Polanyi, J. C. *J. Chem. Phys.* **1980**, *73*, 5895.
- (2) Hering, P.; Brooks, P. R.; Curl, R. F.; Judson, R. S.; Lowe, R. S. *Phys. Rev. Lett.* **1980**, *44*, 687.
- (3) Zewail, A. H. *Science* **1988**, *242*, 1645.
- (4) Neumark, D. M. *Annu. Rev. Phys. Chem.* **1992**, *43*, 153.
- (5) Wenthold, P. G.; Hrovat, D. A.; Borden, W. T.; Lineberger, W. C. *Science* **1996**, *272*, 1456.
- (6) Woodward, R. B.; Hoffmann, R. *J. Am. Chem. Soc.* **1965**, *87*, 395.
- (7) Ribas-Arino, J.; Marx, D. *Chem. Rev.* **2012**, *112*, 5412.
- (8) Caruso, M. M.; Davis, D. A.; Shen, Q.; Odom, S. A.; Sottos, N. R.; White, S. R.; Moore, J. S. *Chem. Rev.* **2009**, *109*, 5755.
- (9) Beyer, M. K.; Clausen-Schaumann, H. *Chem. Rev.* **2005**, *105*, 2921.
- (10) Liang, J.; Fernandez, J. M. *ACS Nano* **2009**, *3*, 1628.
- (11) Wu, D.; Lenhardt, J. M.; Black, A. L.; Akhremitchev, B. B.; Craig, S. L. *J. Am. Chem. Soc.* **2010**, *132*, 15936.
- (12) Hickenboth, C. R.; Moore, J. S.; White, S. R.; Sottos, N. R.; Baudry, J.; Wilson, S. R. *Nature* **2007**, *446*, 423.
- (13) Davis, D. A.; Hamilton, A.; Yang, J.; Cremar, L. D.; Van Gough, D.; Potisek, S. L.; Ong, M. T.; Braun, P. V.; Martinez, T. J.; White, S. R.; Moore, J. S.; Sottos, N. R. *Nature* **2009**, *459*, 68.
- (14) Sheiko, S. S.; Sun, F. C.; Randall, A.; Shirvanyants, D.; Rubinstein, M.; Lee, H.-i.; Matyjaszewski, K. *Nature* **2006**, *440*, 191.
- (15) Basedow, A. M.; Ebert, K. H. *Adv. Polym. Sci.* **1977**, *22*, 83.
- (16) Lenhardt, J. M.; Ong, M. T.; Choe, R.; Evenhuis, C. R.; Martinez, T. J.; Craig, S. L. *Science* **2010**, *329*, 1057.
- (17) Klukovich, H. M.; Kean, Z. S.; Ramirez, A. L. B.; Lenhardt, J. M.; Lin, J.; Hu, X.; Craig, S. L. *J. Am. Chem. Soc.* **2012**, *134*, 9577.
- (18) Lenhardt, J. M.; Ogle, J. W.; Ong, M. T.; Choe, R.; Martinez, T. J.; Craig, S. L. *J. Am. Chem. Soc.* **2011**, *133*, 3222.
- (19) Tian, F.; Lewis, S. B.; Bartberger, M. D.; Dolbier, W. R.; Borden, W. T. *J. Am. Chem. Soc.* **1998**, *120*, 6187.
- (20) Getty, S. J.; Hrovat, D. A.; Xu, J. D.; Barker, S. A.; Borden, W. T. *J. Chem. Soc., Faraday Trans.* **1994**, *90*, 1689.
- (21) Hillmyer, M. A.; Laredo, W. R.; Grubbs, R. H. *Macromolecules* **1995**, *28*, 6311.
- (22) Kuipers, M. W. A.; Iedema, P. D.; Kemmere, M. F.; Keurentjes, J. T. F. *Polymer* **2004**, *45*, 6461.
- (23) Lenhardt, J. M.; Black, A. L.; Craig, S. L. *J. Am. Chem. Soc.* **2009**, *131*, 10818.
- (24) Lenhardt, J. M., *Ph.D. Thesis*, Duke University, 2011.
- (25) Wang, J.; Kouznetsova, T. B.; Niu, Z.; Ong, M. T.; Klukovich, H. M.; Rheingold, A. L.; Martinez, T. J.; Craig, S. L. *Nat. Chem.* **2015**, *7*, 323.

- (26) Ong, M. T.; Leiding, J.; Tao, H. L.; Virshup, A. M.; Martinez, T. *J. Am. Chem. Soc.* **2009**, *131*, 6377.
- (27) Carpenter, B. K. *J. Am. Chem. Soc.* **1996**, *118*, 10329.
- (28) Hrovat, D. A.; Fang, S.; Borden, W. T.; Carpenter, B. K. *J. Am. Chem. Soc.* **1997**, *119*, 5253.
- (29) Piermattei, A.; Karthikeyan, S.; Sijbesma, R. P. *Nat. Chem.* **2009**, *1*, 133.
- (30) Kean, Z. S.; Niu, Z.; Hewage, G. B.; Rheingold, A. L.; Craig, S. L. *J. Am. Chem. Soc.* **2013**, *135*, 13598.
- (31) Larsen, M. B.; Boydston, A. J. *J. Am. Chem. Soc.* **2013**, *135*, 8189.
- (32) Tian, Y.; Kucharski, T. J.; Yang, Q. Z.; Boulatov, R. *Nat. Commun.* **2013**, *4*, 2538.
- (33) Wang, J.; Kouznetsova, T. B.; Kean, Z. S.; Fan, L.; Mar, B. D.; Martínez, T. J.; Craig, S. L. *J. Am. Chem. Soc.* **2014**, *136*, 15162.
- (34) Harris, R. K.; Becker, E. D.; De Menezes, S. M. C.; Goodfellow, R.; Granger, P. *Pure Appl. Chem.* **2001**, *73*, 1795.
- (35) Wu, S.-H.; Liu, W.-Z.; Jiang, X.-K. *J. Org. Chem.* **1994**, *59*, 854.
- (36) Kukovinets, O. S.; Kargapol'tseva, T. A.; Kukovinets, A. G.; Galin, B. Z.; Zorin, V. V.; Tolstikov, G. A. *Russ. J. Org. Chem.* **2000**, *36*, 214.
- (37) Roos, B. O. *Adv. Chem. Phys.* **1987**, *69*, 399.
- (38) Roos, B. O. *Acc. Chem. Res.* **1999**, *32*, 137.